

Histological and Immunohistochemical Study on the Effect of Potassium Bromate on Gastric Fundic Mucosa of Adult Male Albino Rats and the Possible Ameliorating Role of Riboflavin

Amira Fahmy Ali, Seham Ahmed Mohammed Abdel Aziz and Rania Said Emara

Department of Histology, Faculty of Medicine; Menoufia University, Egypt

ABSTRACT

Introduction: Potassium bromate (KBrO₃) is a strong oxidizing agent and utilized as a flour improver. KBrO₃ has Carcinogenic and mutagenic effects, it could generate free radicals and reactive oxygen species (ROS). Potassium bromate is accused as irritating material to tissue surfaces which comes in contact with. Riboflavin has a vital role in cellular function and growth. It possesses a potent antioxidant, anti-inflammatory and immune-modulatory effects.

Objective: Estimate the effect of Potassium bromate on gastric fundic mucosa and the possible ameliorating effect of riboflavin in adult male albino rats.

Material and Methods: Forty adult male albino rats utilized in the current work. The rats were split to control group, Riboflavin-treated group, Potassium bromate-treated group, Potassium bromate and Riboflavin treated group. At the assigned time, the gastric fundic tissues were obtained for biochemical, histological, histochemical and immunohistochemical studies

Results: Potassium bromate treated group exhibited marked deterioration of the fundic mucosa as a wide area of epithelial discontinuity, parietal and chief cells appeared with small darkly stained nuclei. Congested blood vessels, and mononuclear cellular infiltrations were observed. Dilatation of rough endoplasmic reticulum cisternae and confluent secretory granules were detected in chief cells. Statistically, there were a highly significant rise in the mean values of optical density for interleukin 6 (IL6) and mean number of Proliferating cell nuclear antigen (PCNA) positive cells. However, these histological changes were alleviated after riboflavin concomitant administration.

Conclusion: KBrO₃ has been proved to induce structural changes in the fundic mucosa, and these changes can be ameliorated by concomitant administration of riboflavin.

Received: 20 December 2021, **Accepted:** 16 February 2022

Key Words: Fundic mucosa, KBrO₃, PCNA, riboflavin.

Corresponding Author: Amira Fahmy Ali, MD, Department of Histology, Faculty of Medicine; Menoufia University, Egypt, **Tel.:** +20 10 6891 5402, **E-mail:** amirafahmy356@yahoo.com

ISSN: 1110-0559, Vol. 46, No. 2

INTRODUCTION

Potassium bromate (KBrO₃) is a white, odorless, and tasteless crystal. It is utilized as an oxidizing agent in hair products, and as a food additive in flour and cereal also, it is used for the brewing of beer or distillation of spirits. Without KBrO₃ in baking, flours require longer times and water with lower temperature. In the baking process, bromate usually changes to bromine^[1].

In human, KBrO₃ is a potential human carcinogen, while, it is a definite carcinogen in animals. The toxicity of KBrO₃ is a result of an increase in the generation of reactive oxygen species (ROS) and free radicals. These radicals cause tissue damage by reacting with macromolecules that leads to homeostasis imbalance and triggering tissue damage^[2].

The international agency for research on cancer categorized KBrO₃ as a category 2B carcinogenic material for human in 1986, depending on experiments done on experimental animals. So, this finding led to prevention of adding bromate to food by many countries^[3,4].

Workers in some industries may breathe KBrO₃ or have direct skin contact with it, suffering from upper respiratory tract irritation, nausea, vomiting, stomachaches and diarrhea that were reported in some cases. Also, some changes in kidney function and different kidney lesions were observed in lab animals exposed to moderate-to-high oral doses of KBrO₃^[5].

Gastric mucosa is also, affected by KBrO₃ that may cause necrosis or inflammation, even it may cause ulcer formation^[6,7]; and some complications such as gastric wall perforations and hemorrhage^[8]

Riboflavin (vitamin B₂) is one of B vitamins^[9]. Naturally, it is present in various foods and is also, added to food products. The B₂ vitamin is a major element of Flavin mononucleotide (FMN) and Flavin adenine dinucleotide (FAD) coenzymes^[10]. These coenzymes have prominent roles in energy production, growth, and development as well as cellular function and fats, drugs, and steroids metabolism^[11]. Also, they maintain the function of various flavoproteins like, oxidases, dehydrogenases, reductases

and monooxygenases^[12] which play an important role in mitochondrial electron transport chain, β -oxidation of fatty acids, redox homeostasis, branched-chain amino acid catabolism, chromatin remodeling and DNA repair^[13,14].

The importance of riboflavin is multitudinous, it is used for the management of many clinical conditions such as migraine and depression^[15] also it is important for the eye and bone health^[16]. Nevertheless, riboflavin nutritional deficiency is considered a risk factor for some diseases including cancer^[17].

Keeping all that in mind, the present study had been carried out to evaluate the effect of KBrO₃ on the fundic mucosa and the possible beneficial role of riboflavin in adult male rats.

MATERIAL AND METHODS

Drugs and chemicals

Potassium bromate (KBrO₃): It is available as white crystals which is dissolved in distilled water, introduced by Sigma Company (St. Louis, Mo, USA).

Riboflavin (vitamin B₂): It is available as capsules (400mg), dissolved in distilled water and introduced by Sigma company.

Animals

Forty adult male albino rats, 3 months of age and weighing 170-200 g were utilized in the present study. The animals were housed in four stainless steel cages in clean well-ventilated room. Food and water were freely available to the rats. Strict care and hygiene were maintained to keep them in a healthy environment. Animals should be kept for one week before the start of the experiment for acclimatization. All animals' protocols were authorized and observed via the Animal Care Committee of the Research Laboratory of Experimental Animals at Faculty of Medicine, Menoufia university, Egypt.

The animals were split into four equal groups

Group I (control group): was further subdivided into subgroup I.a, the animals kept with no intervention and subgroup I.b, the animals received 10 ml distilled water by oral intubation once daily for 8 weeks.

Group II (Riboflavin-treated group): The animals received riboflavin, 100 mg/kg/d via oral intubation for 8 weeks^[18].

Group III (Potassium bromate-treated group): The animals received KBrO₃, 30 mg/Kg/d, dissolved in 10ml distilled water, via oral intubation for 8 weeks^[19].

Group IV (Potassium bromate and Riboflavin treated group): The animals in this group received KBrO₃ and Riboflavin concomitantly, with the same doses and duration as groups II & III respectively.

24 h after the last dose of drugs administration, ether inhalation was used to anaesthetize the rats from all

groups. The gastric fundic tissue were obtained and processed for biochemical, histological, histochemical and immunohistochemical studies in different study groups.

Biochemical study

Oxidant and Anti-oxidant markers

For determination of oxidant and antioxidant enzymes, gastric tissues were dissected and then homogenized in potassium phosphate buffer solution (50Mm, Ph 7.5) via utilizing a potter Elvehjem homogenizer to allow 10 % homogenate. Homogenate were centrifuged, supernatant was recovered, placed on ice, and the activities of Superoxide dismutase (SOD)^[20] as well as the contents of Glutathione (GSH)^[21] and Malondialdehyde (MDA)^[22] were detected.

Histological study

The tissue samples were fixed in 10% buffered formalin and processed for paraffin blocks. Then, sections of 5-7 μ m thickness were cut and stained with hematoxylin & eosin (Hx&E) to observe the histological structure and Mallory trichrome (M.T) stain to detect the collagen fibers^[23].

Transmission electron microscopic study

Small pieces of the gastric fundic mucosa from all animal groups were rapidly fixed in 3% glutaraldehyde solution and processed for examination, utilizing a Joel electron microscope. TEM processing and analysis were carried out at the E.M Center, faculty of Medicine, Tanta University^[24].

Histochemical study

The specimens were processed and stained with Alcian blue for detection of mucopolysaccharides^[25].

Immunohistochemical study

- Immunohistochemical study of Interleukin 6 (IL6) (a marker of inflammation): The primary monoclonal antibody was the mouse anti-IL6 (1:2000 dilution, Lab Vision Clone 6B4/GH 54; Santa Cruz Biotechnology Inc., USA). Negative control sections were processed by replacing the primary antibody with buffer alone. Skin was utilized as a positive control. The positive reaction was cytoplasmic brown color^[26]. Counterstaining was performed using Mayer's hematoxylin.
- Immunohistochemical study of anti-proliferating cell nuclear antigen (PCNA): The mouse anti-PCNA monoclonal antibody was used as the primary monoclonal antibody (1:3000 dilution, Santa Cruz Biotechnology, USA). PCNA is used as the most reliable immunohistochemical marker for evaluating cell proliferation. Negative control sections were processed by replacing the primary antibody with buffer alone. Lymph node was utilized as a positive control. Nuclear staining with brown color was considered as a positive reaction^[27].

Morphometrical study

The thickness of gastric fundic mucosa was measured in Hx&E sections. The area percentages of collagen fibers in Mallory' trichrome stained sections and positive mucus cells in Alcian blue sections, optical density of IL6 and number of PCNA positive cells in immunostained sections were measured, utilizing the objective lens of magnification X40. For each group, five slides of five different specimens were examined. From each slide, ten non-overlapping fields were measured in a standard measuring frame. This was performed utilizing the interactive measuring menu of image analyzer (LeciaQwin 500 image analyzer computer system, England) in anatomy department, faculty of medicine, Menoufia University.

Assessment of gastric mucosal lesion (ulcer index)

The lesions in the gastric mucosa were expressed in the term of ulcer index (UI) depending on the calculation of lesion index utilizing 0-5 scoring system according to the severity and number of gastric lesions. Severity factor: 0 = no lesions; 1 = small round hemorrhagic lesions; 2 = lesions <2 mm; 3 = lesions 2–3 mm; 4 = lesions 3–4 mm; 5 = lesion > 4 mm. The score was multiplied by 2 when the width of the erosion is larger than 1mm. The mean score was calculated and expressed as the UI^[28].

Statistical analysis

The collected data were analyzed and compared by student's t-test. The P-value was utilized to test the significant changes in each parameter in comparison with the control group. Then, the data were expressed as mean \pm SD and analyzed utilizing statistical package for the Social Science Software (SPSS) (V. 17.0 for windows; SPSS Inc., Illinois, USA). *P value* set at 0.05, *P*>0.05 non-significant, *P value*<0.05 significant^[29].

RESULTS

Biochemical results

Group II (riboflavin treated group) demonstrated a non-significant change in the MDA (lipid peroxidation marker), GSH and SOD (antioxidant enzyme) levels in comparison with control animals (*P*>0.05). Group III (KBrO₃ treated group) displayed a highly significant increase in the MDA level (*P*<0.001) and a significant decrease in the GSH and SOD levels in comparison with the animals of control group (*P*<0.05). Moreover, group IV (KBrO₃ and riboflavin treated group) exhibited a non-significant change in the mean values of MDA, GSH and SOD (*P*>0.05) when compared with the control animals, while revealed a highly significant decrease in the MDA level (*P*<0.001), also, revealed a significant increase in the antioxidant enzymes level (*P*<0.05) in comparison with KBrO₃ treated group (Table 1, Histograms 1a,1b,1c).

Histological results

Hx&E sections of the fundic mucosa of stomach of control group (group I) revealed normal histological

fundic mucosa structure, composed of fundic glands, lamina propria and finally muscularis mucosa. The lamina propria was occupied by closely packed tubular fundic glands which were perpendicular to the surface. Each gland was differentiated to isthmus which open to the surface by short pits, middle part called neck and basal regions, resting on muscularis mucosa (Figure 1). The lining epithelium consisted of surface columnar cells which had pale cytoplasm and basal oval nuclei. Mucus neck cells had basal flattened nuclei (Figure 2). Parietal cells appeared polyhedral with central rounded vesicular nuclei and deeply acidophilic cytoplasm. The chief cells appeared pyramidal with basal rounded vesicular nuclei and basophilic cytoplasm (Figure 3). Gastric pits and intact mucus coat were observed (Figure 2). Sections of the fundic mucosa of stomach of riboflavin treated group (groups II) showed no structural changes and the pictures were similar to control group.

Group III (KBrO₃ treated group) exhibited histological mucosal alterations. There was widening of gastric pits. The upper parts of fundic glands were lined by flattened epithelial cells. Extravasation of red blood cells was seen (Figure 4). Desquamation and sloughing of the surface epithelial cells (Figures 4,5,6), a wide area of epithelial discontinuity (Figure 5) and ulceration extending down to muscularis mucosa (Figure 6) were noticed. Parietal cells displayed small deeply stained nuclei; others appeared with karyolytic changes with vacuolated cytoplasm. The chief cells showed deep basophilic cytoplasm and small darkly stained nuclei. Some areas showed cellular loss (Figure 7). However, congested blood vessels (Figure 8), and mononuclear cellular infiltrations in the lamina propria were evident (Figures 4,6,8).

Sections of the of group IV (KBrO₃ and riboflavin treated group) revealed nearly normal gastric fundic glands. Surface columnar cells and mucus neck cells were nearly similar to control but there is no mucous coat and small deeply stained nuclei was seen (Figure 9). Parietal cells displayed central rounded vesicular nuclei and acidophilic cytoplasm. The chief cells showed basal rounded vesicular nuclei and basophilic cytoplasm (Figure 10).

Gastric fundic mucosa stained with Mallory trichrome in control group (group I) displayed few amounts of collagen fibers in the lamina propria (Figure 11). While group III (KBrO₃ treated group) was appeared with apparent increase in the amount of collagen fibers (Figure 12). Moreover, group IV (KBrO₃ and riboflavin treated group) revealed apparent decreased in the amount of collagen fibers as compared to group III (Figure 13).

Ultra-thin sections of the fundic tissue of control rats (group I) exhibited mucus neck cell with basal flat euchromatic nucleus and prominent nucleolus, Golgi apparatus and numerous apical electron lucent secretory mucus granules (Figure 14). The parietal cell had central rounded euchromatic nucleus, numerous rounded mitochondria, well developed tubulovesicular

system and rough endoplasmic reticulum cisternae (Figure 15). Moreover, the chief cell revealed basal rounded euchromatic nucleus with prominent nucleolus and perinuclear space. Its cytoplasm contained apical electron lucent zymogen granules, mitochondria and parallel cisternae of rough endoplasmic reticulum (Figure 16). An enteroendocrine cell displayed rounded euchromatic nucleus and small electron dense granules, mitochondria, lysosome and cisternae of rough endoplasmic reticulum (Figure 17). An electron microscopic examination of Group II (riboflavin treated group) showed no visible dissimilarity from the control group. While, an electron microscopic examination of Group III (KBrO₃ treated group) revealed mucus neck cell with basal heterochromatic nucleus and wide perinuclear space, apical fused electron lucent secretory mucus granules, mitochondria and of rough endoplasmic reticulum cisternae (Figure 18). The parietal cell had flat irregular heterochromatic nucleus and the cytoplasm contained disturbed tubulovesicular system, degenerated mitochondria and lysosome. Collagen fibers were also seen (Figure 19). The chief cell exhibited nucleus with peripheral condensation of chromatin and wide perinuclear space, dilated cisternae of rough endoplasmic reticulum, confluent electron lucent zymogen granules and mitochondria (Figure 20). While, an enteroendocrine cell had shrunken irregular heterochromatic nucleus with karyolytic changes, cytoplasmic vacuoles, few small electron dense granules and degenerated mitochondria (Figure 21).

Moreover, an electron microscopic examination of the Group IV (KBrO₃ and riboflavin treated group) revealed preservation of gastric fundic tissue. The mucus neck cell had basal flat euchromatic nucleus with prominent nucleolus, apical electron lucent secretory granules, mitochondria and rough endoplasmic reticulum cisternae (Figure 22). The parietal cell displayed oval to round central euchromatic nucleus, numerous mitochondria and well developed tubulovesicular system (Figure 23). The chief cell had basal rounded euchromatic nucleus and prominent nucleolus. The cytoplasm contained apical electron lucent zymogen granules, mitochondria and parallel cisternae of rough endoplasmic reticulum (Figure 24). While, an enteroendocrine cell showed slightly irregular euchromatic nucleus and the cytoplasm contained small electron dense granules and mitochondria (Figure 25).

Histochemical results

Regarding to Alcian blue (AB) reaction, gastric fundic mucosa of control group (group I) displayed strong reaction in the mucus coat which extends to fill gastric pits and mucus neck cells (Figure 26). Moreover, group III (KBrO₃ treated group) revealed mild AB reaction in the mucus neck cells (Figure 27). While, group IV (KBrO₃ and riboflavin treated group) revealed moderate AB reaction in the mucus coat which extends to fill gastric pits and mucus neck cells (Figure 28).

Immunohistochemical results

Regarding IL6 immune-marker expression, gastric fundic mucosa of control group (group I) revealed minimal cytoplasmic immunoreactivity for IL6 in the glandular cells (Figure 29). Group III (KBrO₃ treated group) revealed strong positive cytoplasmic immunoreactivity for IL6 in the glandular cells (Figure 30). While, group IV (KBrO₃ and riboflavin treated group) revealed moderate cytoplasmic immunoreactivity for IL6 (Figure 31).

Regarding PCNA immune-marker expression, gastric fundic mucosa of control group (group I) revealed a few number of positive PCNA immunoreactivity in the glandular cells (Figure 32). Group III (KBrO₃ treated group) displayed increase in the number of positive nuclear PCNA immunoreactivity in the glandular cells (Figure 33). While, group IV (KBrO₃ and riboflavin treated group) revealed decreased positive nuclear PCNA immunoreactivity as compared to group III (Figure 34).

Morphometric and statistical results

Data in (Table 2) demonstrated that group III (KBrO₃ treated group) exhibited a highly significant decrease in mucosal thickness and a highly significant increase in ulcer index in comparison with the control rats ($P < 0.001$), while group IV (KBrO₃ and riboflavin treated group) displayed non-significant changes in these parameters in comparison with the control animals ($P > 0.05$) and a highly significant changes ($P < 0.001$) in comparison with KBrO₃ treated rats (group III) (Histograms, 2a,2b).

Data in (Table 3) showed that group III (KBrO₃ treated group) exhibited a highly significant rise in the mean area percentage of collagen fibers deposition, mean values of optical density for IL6 and mean number of PCNA positive cells and exhibited a highly significant decrease in mean values of Alcian blue Positive mucus cells ($P < 0.001$) when compared with the control animals. Moreover, group IV (KBrO₃ and riboflavin treated group) displayed significant changes, in these parameters when compared with the control groups ($P < 0.05$) and a highly significant changes when compared with KBrO₃ group (Histograms 3a, 3b, 3c,3d).

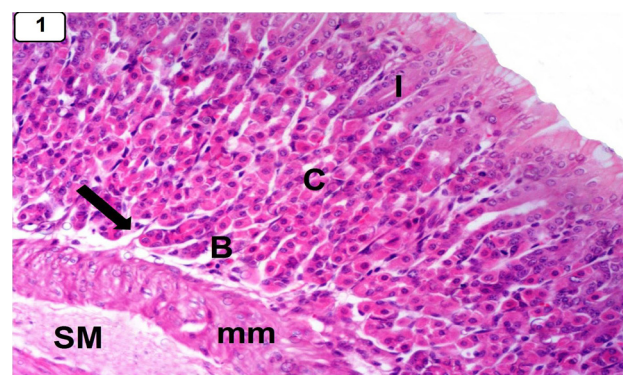


Fig. 1: A photomicrograph of a gastric fundic mucosa of control group illustrating closely packed tubular fundic glands resting on muscularis mucosa (mm). The fundic glands are composed of isthmus (I), neck (C) and base (B). Notice, the lamina propria (black arrow) and submucosa (SM). Hx&E X100

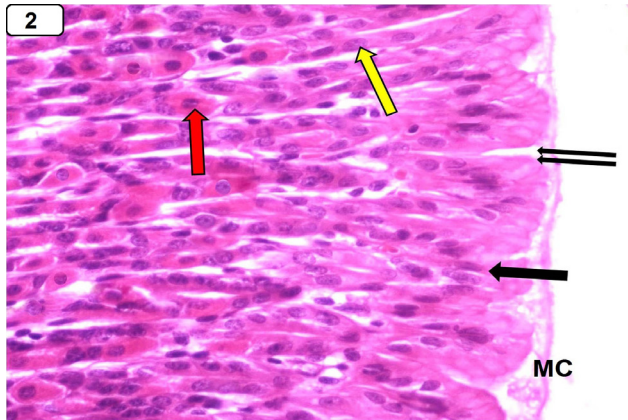


Fig. 2: A photomicrograph of a gastric fundic mucosa of control group illustrating surface columnar cells with pale cytoplasm and basal oval nuclei (black arrow), mucus neck cells have basal flattened nuclei (yellow arrow) lining the upper part of fundic glands. Parietal cells (red arrow) are observed. Gastric pits (double arrow) and intact mucus coat (MC) are seen. Hx&E X200

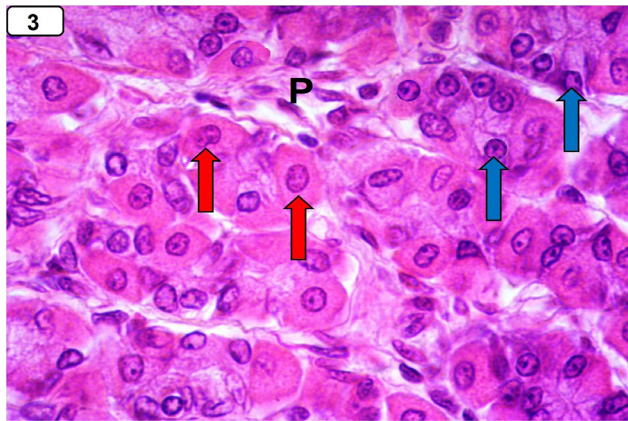


Fig. 3: A photomicrograph of a gastric fundic mucosa of control group illustrating the lower part of fundic glands. The parietal cells are polyhedral in shape with deeply acidophilic cytoplasm and central rounded vesicular nuclei (red arrows). Chief cells are pyramidal in shape with basophilic cytoplasm and basal rounded vesicular nuclei (blue arrows). Notice, lamina propria (P) between the fundic gastric glands. Hx&E X400

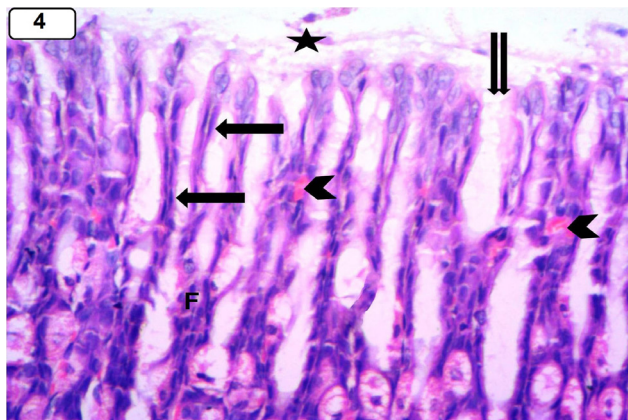


Fig. 4: A photomicrograph of a gastric fundic mucosa of KBrO3 treated group illustrating exfoliated cells (star) within gastric lumen and wide gastric pits (double arrow). The upper parts of fundic glands are lined by flattened epithelial cells (black arrows). Extravasation of red blood cells (arrow head) and mononuclear cellular infiltrations (F) in lamina propria are seen. Hx&E X200

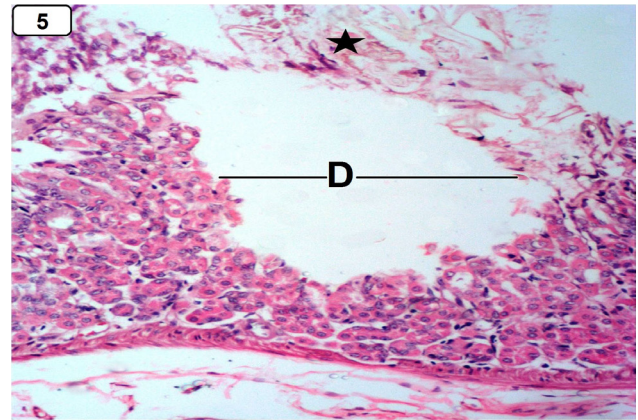


Fig. 5: A photomicrograph of a gastric fundic mucosa of KBrO3 treated group illustrating a wide area of epithelial discontinuity (D). Sloughed epithelial cells are seen in the lumen (star). Hx&E X100

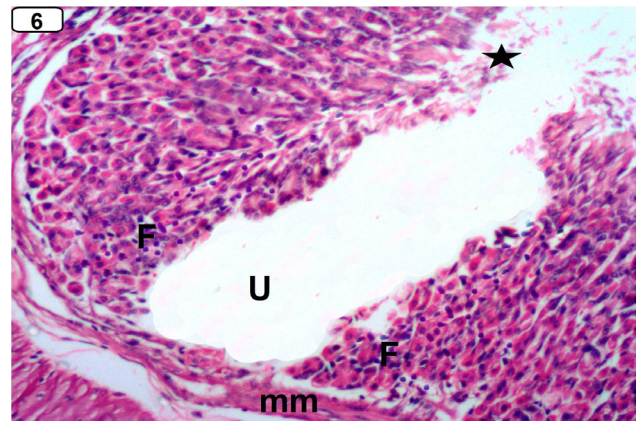


Fig. 6: A photomicrograph of a gastric fundic mucosa of KBrO3 treated group illustrating ulceration (U) extending down to muscularis mucosa (mm) and mononuclear cellular infiltrations (F) in the lamina propria. Sloughed epithelial lining (star) are seen. Hx&E X100

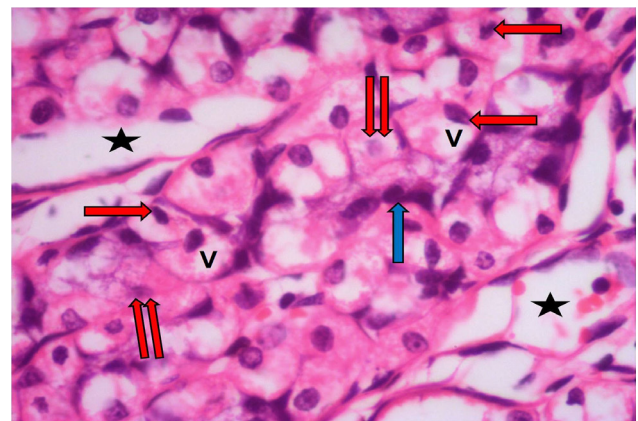


Fig. 7: A photomicrograph of a gastric fundic mucosa of KBrO3 group illustrating parietal cells with vacuolated cytoplasm (V) and small deeply stained nuclei (red arrows), others have karyolytic nuclear alterations (red double arrows). The chief cells appear with deep basophilic cytoplasm and small darkly stained nuclei (blue arrow). Some areas show cellular loss (star). Hx&E X400

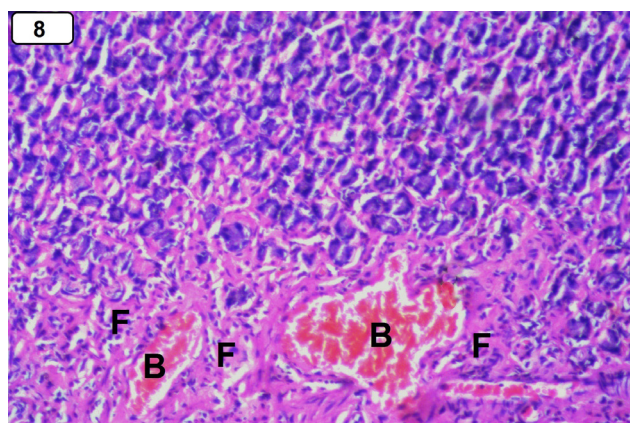


Fig. 8: A photomicrograph of a gastric fundic mucosa of KBrO3 treated group illustrating congested blood vessels (B), and mononuclear cellular infiltrations (F). Hx&E X100

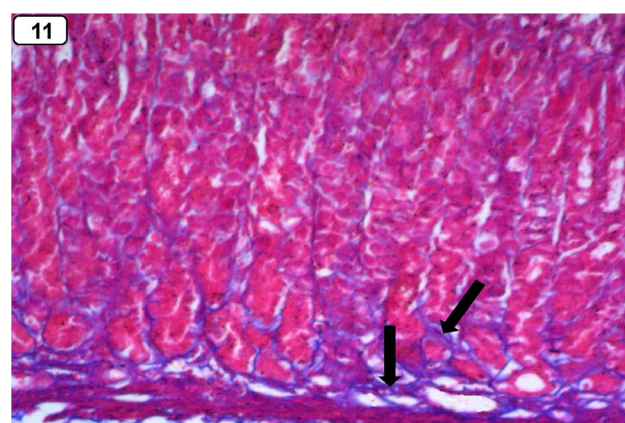


Fig. 11: A photomicrograph of a gastric fundic mucosa of control group illustrating few amount of collagen fibers in the lamina propria (arrows). M.T X100

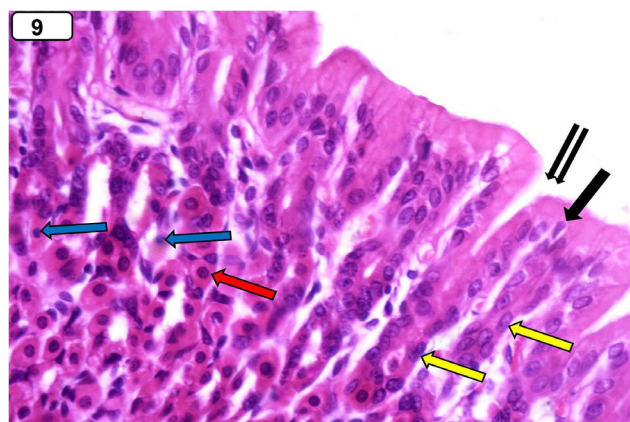


Fig. 9: A photomicrograph of a gastric fundic mucosa of KBrO3 and riboflavin treated group illustrating gastric pits (black double arrows). Surface columnar cells (black arrow), mucus neck cells (yellow arrows) and parietal cells (red arrow) are nearly similar to control. Notice, no mucous coat and small deeply stained nuclei (blue arrows). Hx&E X200

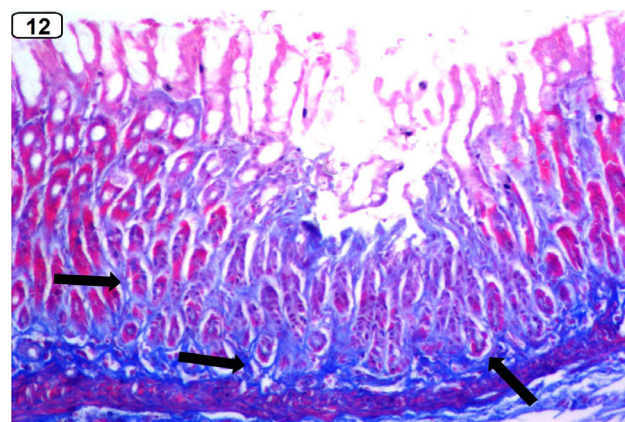


Fig. 12: A photomicrograph of a gastric fundic mucosa of KBrO3 treated group illustrating apparent increase in the amount of collagen fibers in the lamina propria (arrows). M.T X100

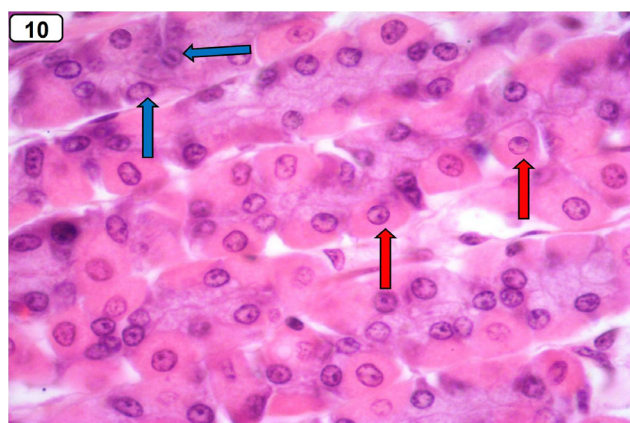


Fig. 10: A photomicrograph of a gastric fundic mucosa of KBrO3 and riboflavin treated group illustrating parietal cells with acidophilic cytoplasm and central rounded vesicular nuclei (red arrows). The chief cells appear with basophilic cytoplasm and basal rounded vesicular nuclei (blue arrows). Hx&E X400

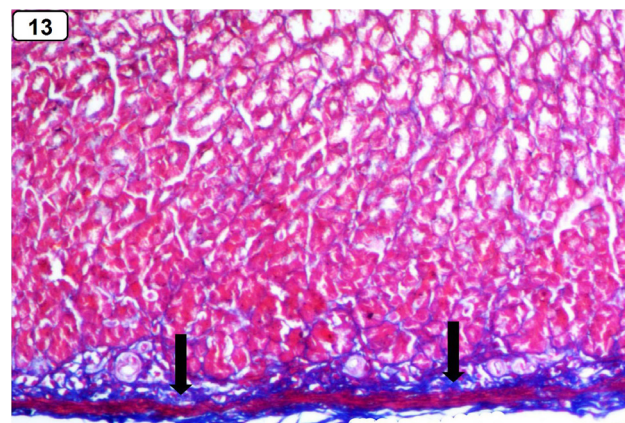


Fig. 13: A photomicrograph of a gastric fundic mucosa of KBrO3 and riboflavin treated group illustrating apparent decreased in the amount of collagen fibers as compared to group III (arrows) M.T X100

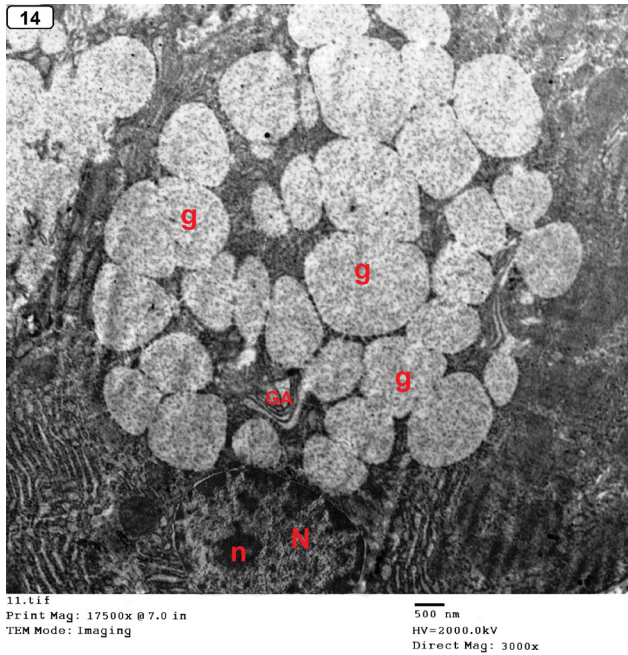


Fig. 14: An electron micrograph of a mucus neck cell of control group illustrating basal flat euchromatic nucleus (N) with prominent nucleolus (n), Golgi apparatus (GA) and numerous apical electron lucent secretory mucus granules(g). X3000

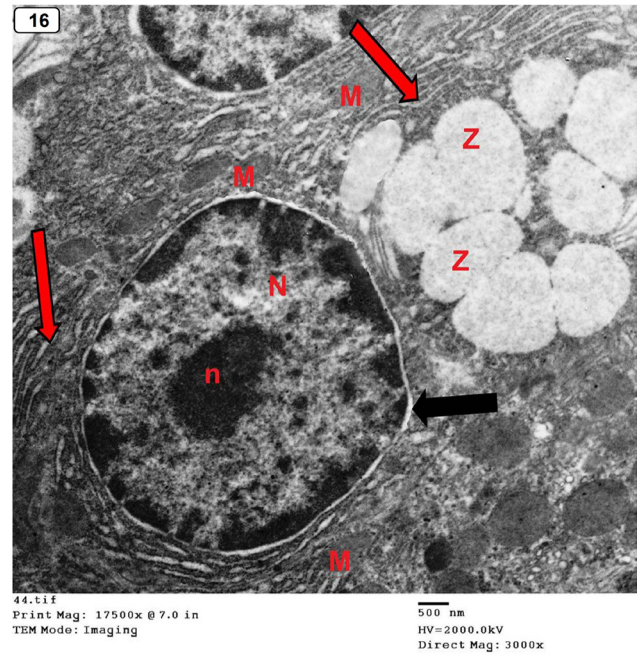


Fig. 16: An electron micrograph of a chief cell of control group illustrating basal rounded euchromatic nucleus (N), prominent nucleolus (n) and perinuclear space (black arrow). The cytoplasm contains apical electron lucent zymogen granules (Z), parallel cisternae of rough endoplasmic reticulum (red arrow) and mitochondria (M). X3000

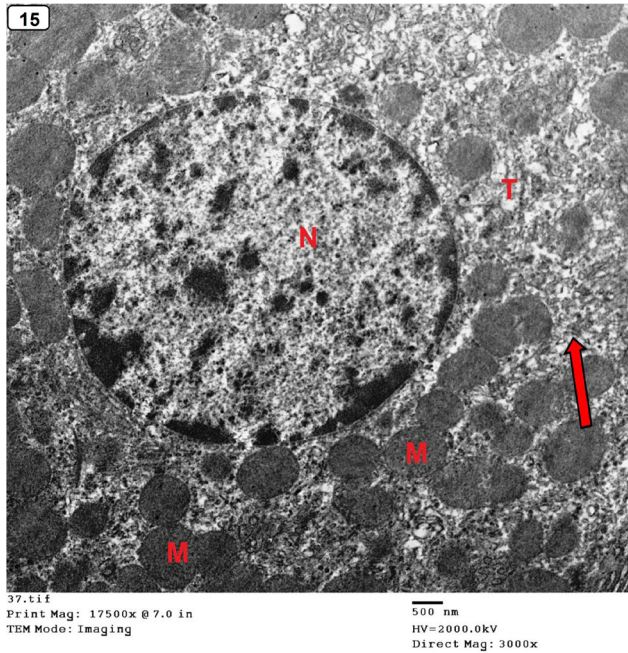


Fig. 15: An electron micrograph of a parietal cell of control group illustrating central rounded euchromatic nucleus (N). The cytoplasm contains numerous rounded mitochondria (M), well developed tubulovesicular system (T) and cisternae of rough endoplasmic reticulum (red arrow). X3000

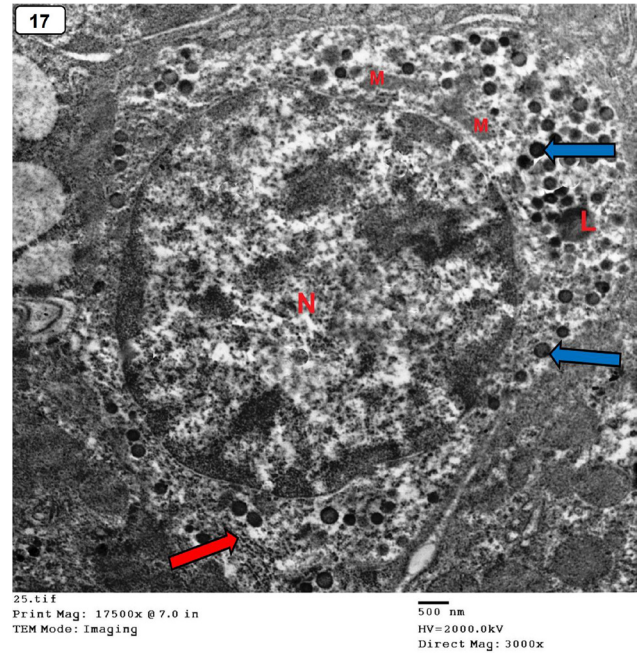


Fig. 17: An electron micrograph of an enteroendocrine cell of control group illustrating rounded euchromatic nucleus (N) and small electron dense granules (blue arrows), mitochondria (M), lysosome (L) and cisternae of rough endoplasmic reticulum (red arrow). X3000

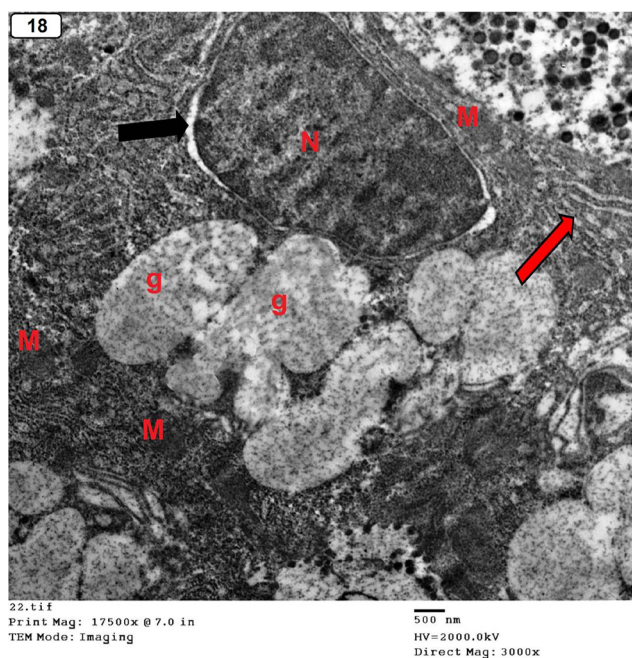


Fig. 18: An electron micrograph of a mucus neck cell of KBrO3 treated group illustrating basal heterochromatic nucleus (N) with wide perinuclear space (black arrow), apical fused electron lucent secretory mucus granules (g), cisternae of rough endoplasmic reticulum (red arrow) and mitochondria (M). X3000



Fig. 20: An electron micrograph of a chief cell of KBrO3 treated group illustrating nucleus (N) with peripheral condensation of chromatin and wide perinuclear space (black arrow), dilated cisternae of rough endoplasmic reticulum (red arrow), confluent electron lucent zymogen granules (Z) and mitochondria (m). X3000

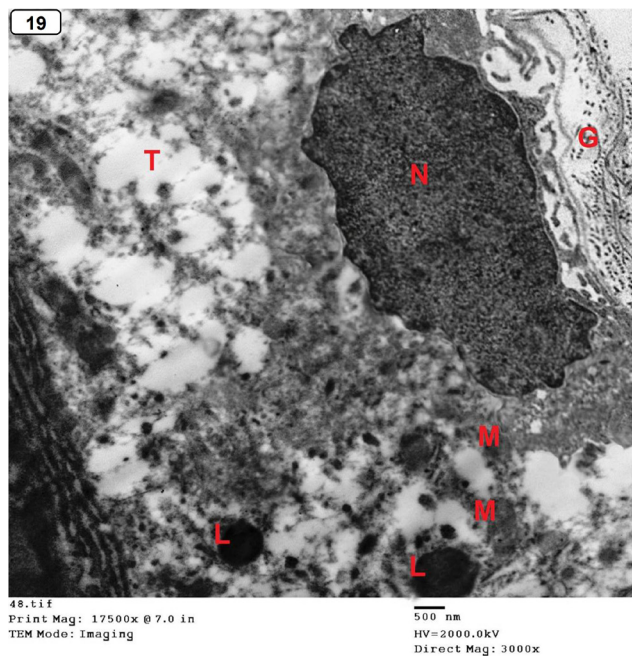


Fig. 19: An electron micrograph of a parietal cell of group KBrO3 treated group illustrating flat irregular heterochromatic nucleus (N). The cytoplasm contains disturbed tubulovesicular system (T), degenerated mitochondria (M) and lysosome (L). Collagen fibers are also seen (G). X3000

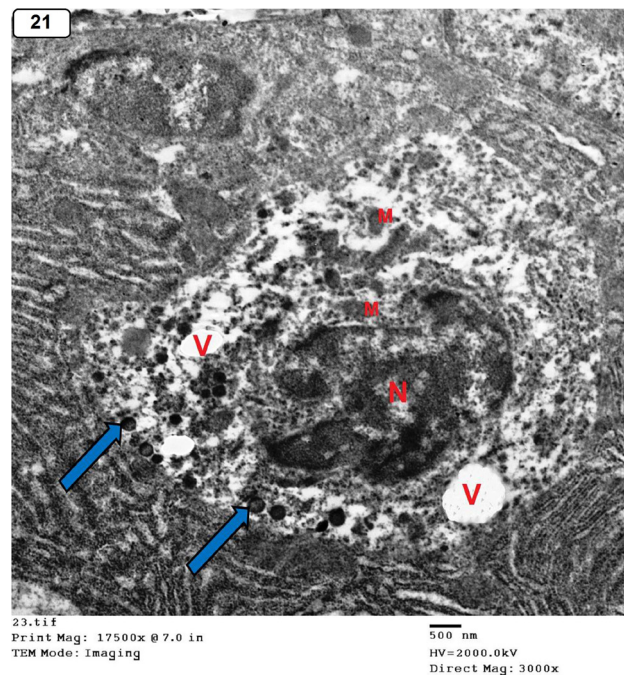


Fig. 21: An electron micrograph of an enteroendocrine cell of KBrO3 treated group illustrating shrunken heterochromatic nucleus with karyolytic changes (N), cytoplasmic vacuoles (V), few small electron dense granules (blue arrows) and degenerated mitochondria (M). X3000

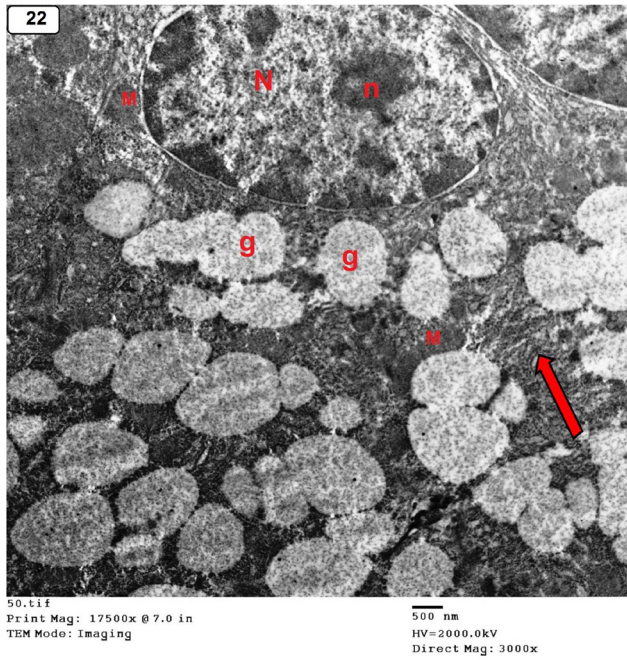


Fig. 22: An electron micrograph of a mucus neck cell of group KBrO₃ and riboflavin treated group illustrating basal flat euchromatic nucleus (N) with prominent nucleolus (n), apical electron lucent secretory granules (g), mitochondria (M) and rough endoplasmic reticulum cisternae (red arrow). X3000

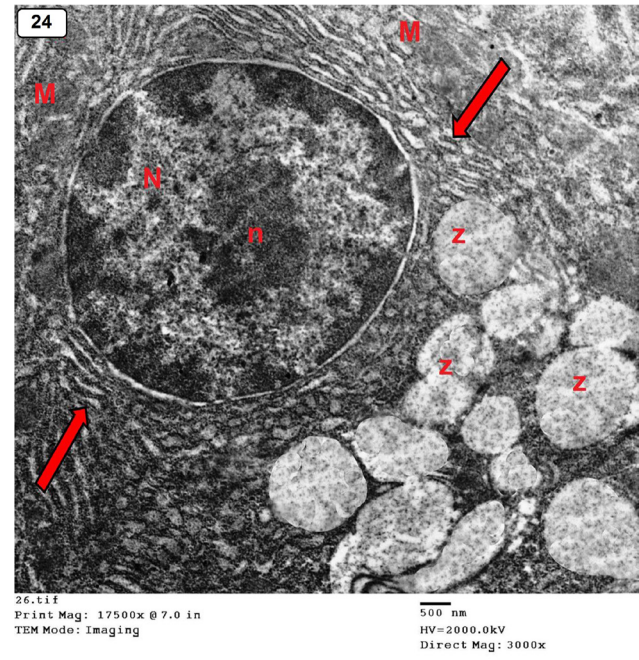


Fig. 24: An electron micrograph of a chief cell of KBrO₃ and riboflavin treated group illustrating basal rounded euchromatic nucleus (N) and prominent nucleolus (n). The cytoplasm contains apical electron lucent zymogen granules (Z), parallel cisternae of rough endoplasmic reticulum (red arrows) and mitochondria (M). X3000

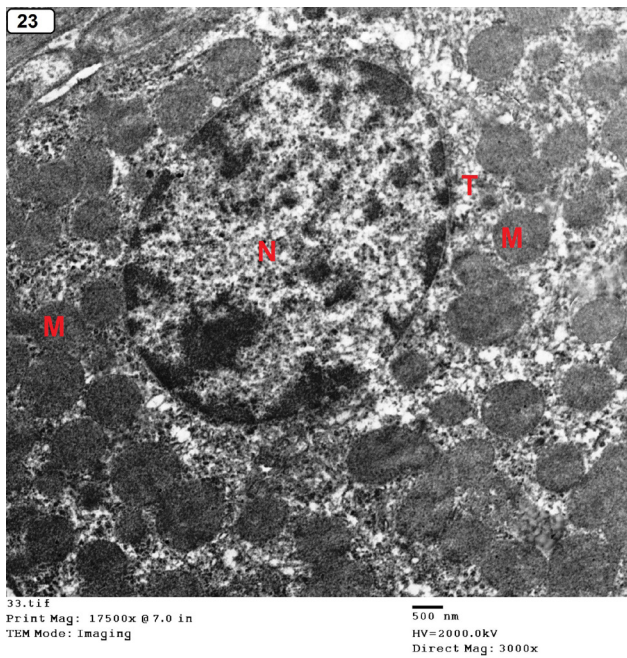


Fig. 23: An electron micrograph of a parietal cell of group KBrO₃ and riboflavin treated group illustrating oval to round central euchromatic nucleus (N), numerous mitochondria (M) and well developed tubulovesicular system (T). X3000

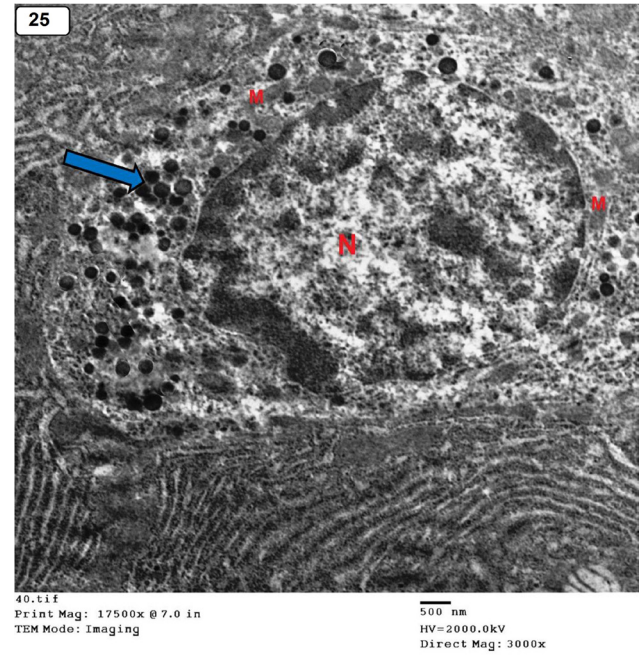


Fig. 25: An electron micrograph of an enteroendocrine cell of KBrO₃ and riboflavin treated group illustrating slightly irregular euchromatic nucleus (N). The cytoplasm contains small electron dense granules (blue arrow) and mitochondria (M). X3000

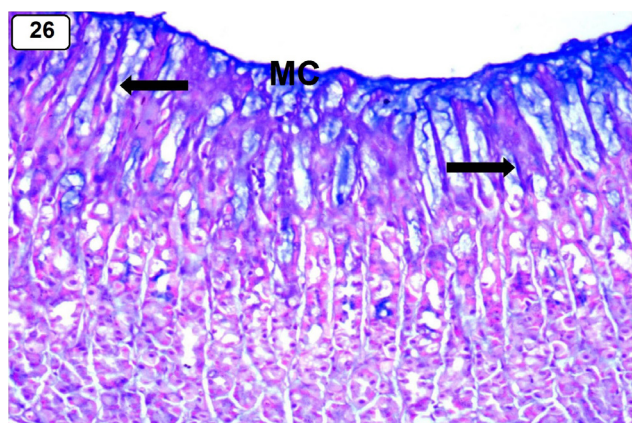


Fig. 26: A photomicrograph of a gastric fundic mucosa of control group illustrating strong AB reaction in the mucus coat (MC) which extends to fill gastric pits and mucus neck cells (arrows). AB X100

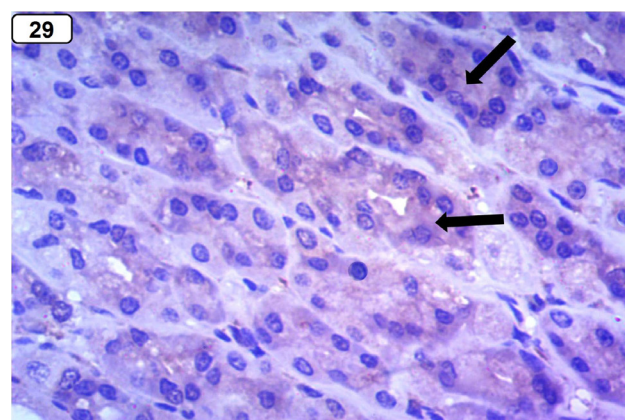


Fig. 29: A photomicrograph of a gastric fundic mucosa of control group illustrating minimal cytoplasmic immunoreactivity for IL6 in the glandular cells (arrows).IL6 X400

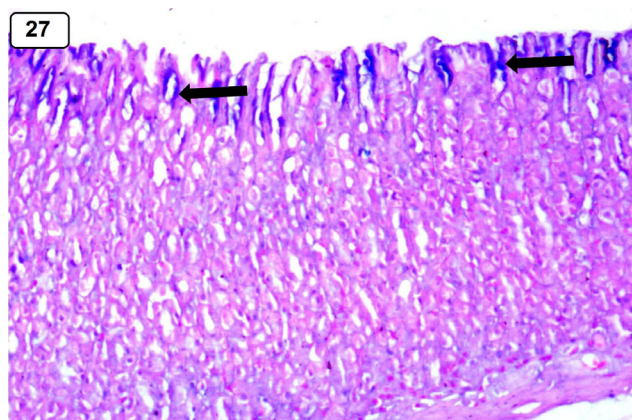


Fig. 27: A photomicrograph of a gastric fundic mucosa of KBrO3 treated group illustrating mild AB reaction in the mucus neck cells (arrows) AB X100

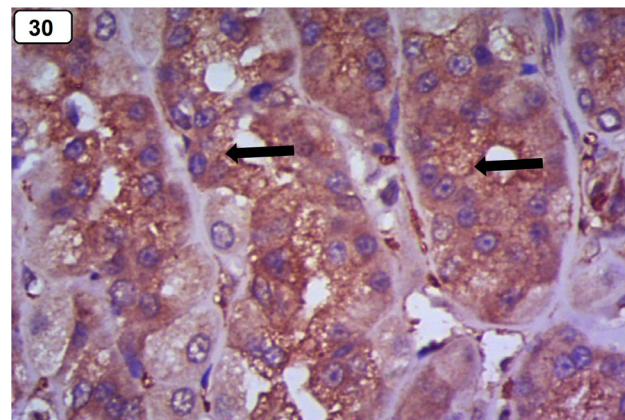


Fig. 30: A photomicrograph of a gastric fundic mucosa of KBrO3 treated group illustrating strong positive cytoplasmic immunoreactivity for IL6 in the glandular cells (arrows). IL6 X400

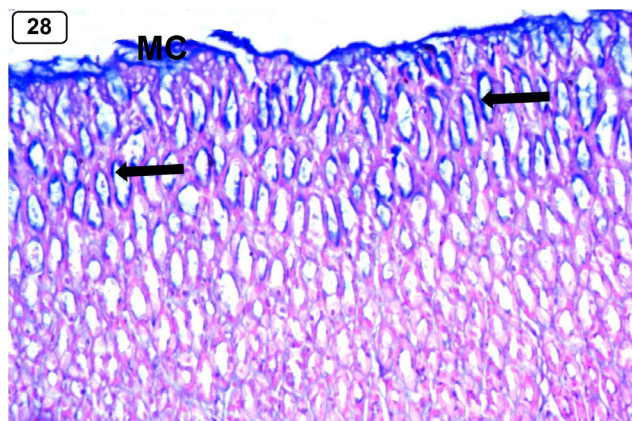


Fig. 28: A photomicrograph of a gastric fundic mucosa of KBrO3 and riboflavin treated group illustrating moderate AB reaction in the mucus coat (MC) which extends to fill gastric pits and mucus neck cells (arrows). AB X100

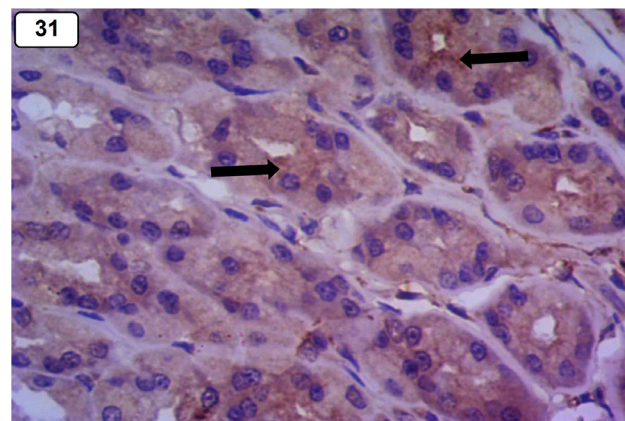


Fig. 31: A photomicrograph of a gastric fundic mucosa of KBrO3 and riboflavin treated group illustrating moderate cytoplasmic immunoreactivity for IL6 in the glandular cells (arrows). IL6 X400

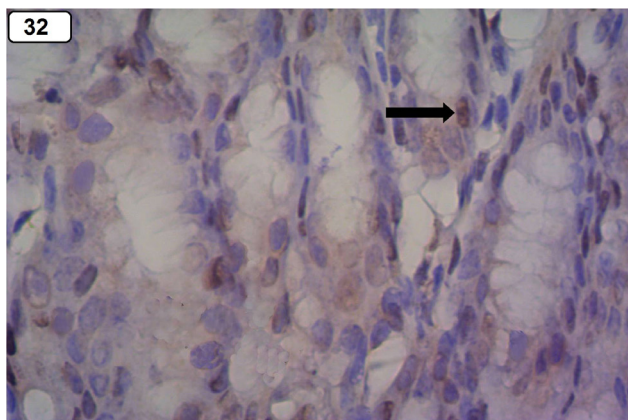


Fig. 32: A photomicrograph of a gastric fundic mucosa of control group illustrating a few number of positive PCNA immunoreactivity in the glandular cells (arrow). PCNA X400

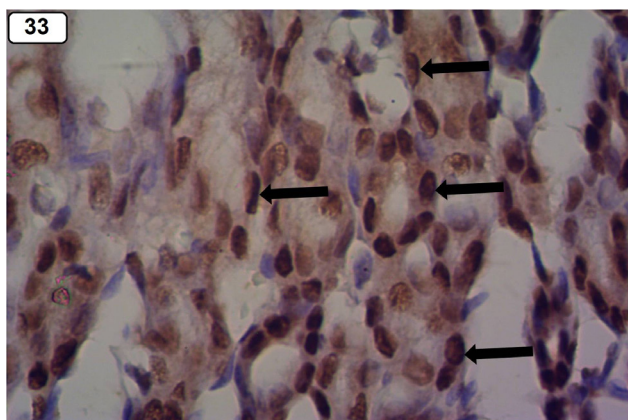


Fig. 33: A photomicrograph of a gastric fundic mucosa of KBrO3 treated group illustrating an increase in the number of positive nuclear PCNA immunoreactivity in the glandular cells (arrows). PCNA X400

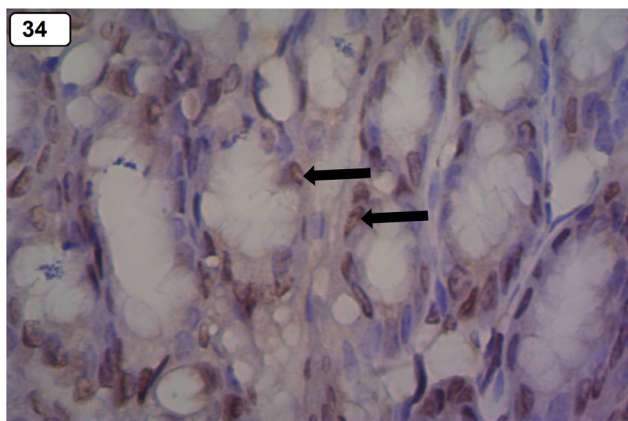


Fig. 34: A photomicrograph of a gastric fundic mucosa of KBrO3 and riboflavin treated group illustrating apparent decreased positive nuclear PCNA immunoreactivity in the glandular cells as compared to group III (arrows). PCNA X400

Table 1: Mean values (M) ± SD of MDA, GSH and SOD in gastric tissue of all groups

| | I | II | III | IV | |
|---------------|----------|----------|-----------|----------|--|
| MDA (nmol/mg) | 2.1±0.4 | 2.5±0.5 | 9.8±1 | 3±1.4 | P1=.106 P2=.000 P3=.084 P4=.000 |
| GSH (umol/g) | 70.5±2 | 72±2.5 | 62.7±7.4 | 69.8±2.8 | P1=.158 P2=.005 P3=.305 P4=.022 |
| SOD (u/mg) | 68.8±2.6 | 68.2±2.2 | 51.3±14.6 | 65.8±5.2 | P1=.549 P2=.002 P3=.116 P4=.013 |

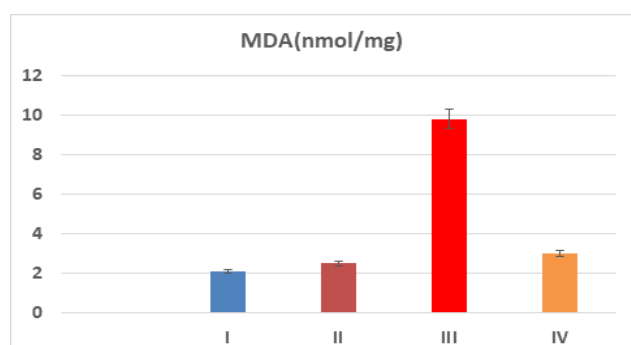
M= the mean value. SD= the standard deviation

Table 2: Mean values±SD of mucosal thickness and ulcer index (UI) in different experimental groups

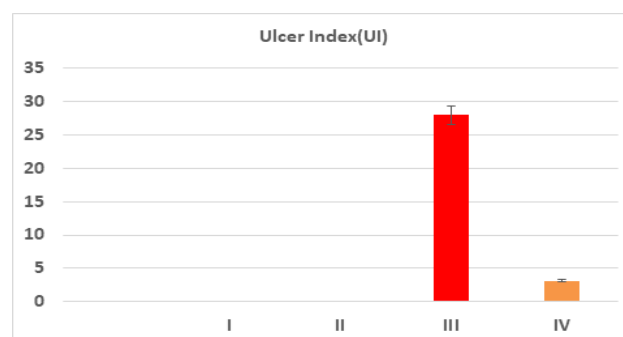
| | I | II | III | IV | |
|-----------------------|-----------|-----------|---------|-----------|--|
| Mucosal thickness (µ) | 252.1±2.7 | 250.2±3.9 | 237±6.2 | 249.7±2.7 | P1=.219 P2=.000 P3=.062 P4=.000 |
| Ulcer index (UI) | 0.00±0.00 | 0.00±0.00 | 28±2.85 | 3.13±1.56 | P1=.552 P2=.000 P3=.077 P4=.000 |

Table 3: Mean area percentage (%) of collagen deposition, alcian blue positive mucus cells, optical density of IL6 and mean number of PCNA +ve cells in different experimental groups

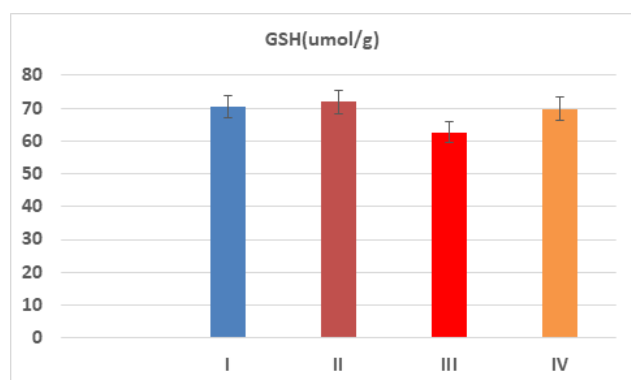
| | I | II | III | IV | |
|------------------------------------|----------|----------|----------|----------|--|
| collagen fibers % | 2±0.5 | 2.3±0.4 | 10.2±1.5 | 4.2±1.9 | P1=.122 P2=.000 P3=.002 P4=.000 |
| Alcian blue Positive mucus cells % | 8.8±0.9 | 8.7±0.8 | 4.5±1.2 | 8±1 | P1=.861 P2=.000 P3=.013 P4=.000 |
| Optical density of IL6 | 0.2±1.8 | 0.3±2.5 | 10.5±1.8 | 2.4±2.1 | P1=.399 P2=.000 P3=.004 P4=.000 |
| Mean number of PCNA +ve cells | 39.3±1.2 | 38.8±1.7 | 80.7±7.3 | 44.8±6.5 | P1=.439 P2=.000 P3=.018 P4=.000 |



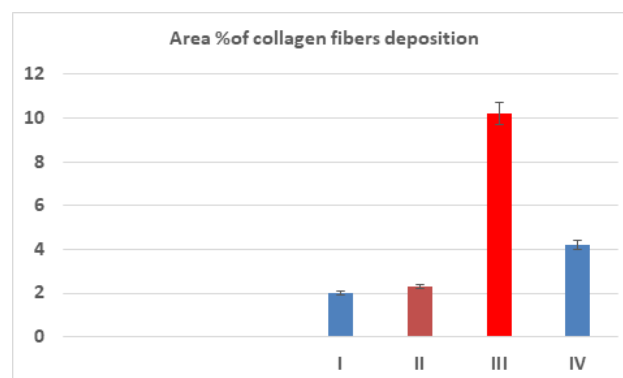
Histogram 1a: Mean values of MDA level in different experimental groups



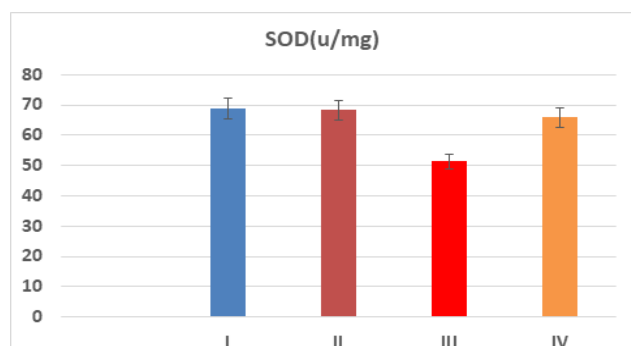
Histogram 2b: Mean values of ulcer index in different experimental group



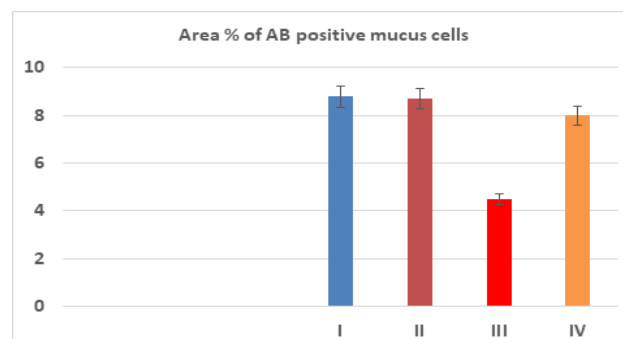
Histogram 1b: Mean values of GSH level in different experimental groups



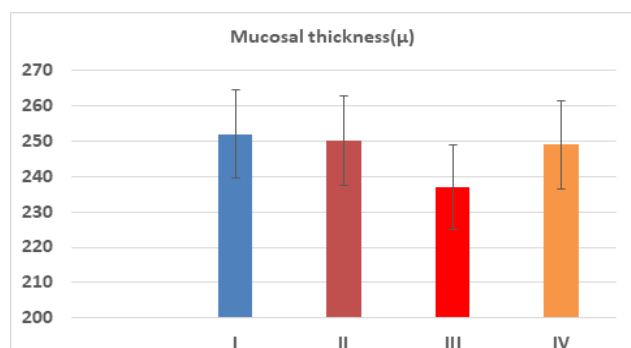
Histogram 3a: Mean area % of collagen fibers deposition in different experimental groups



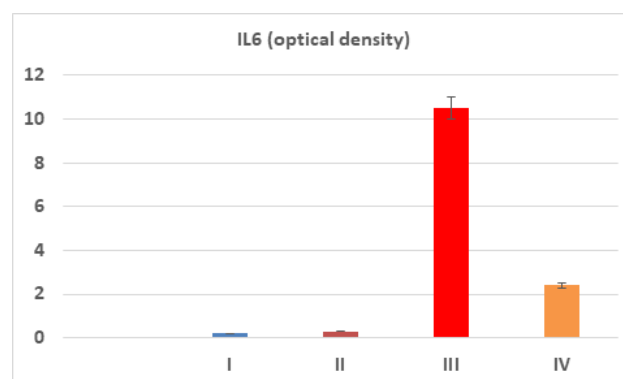
Histogram 1c: Mean values of SOD level in different experimental groups



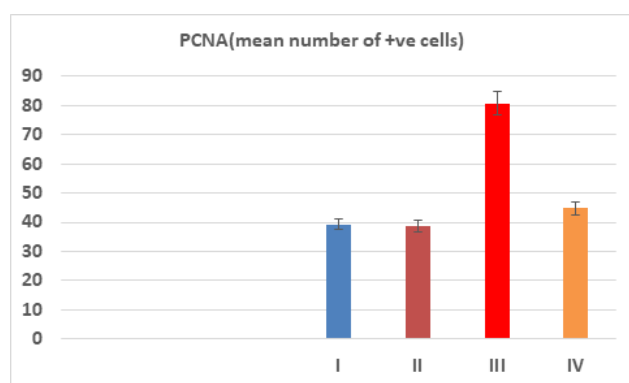
Histogram 3b: Mean area % of AB positive mucus cells in different experimental groups



Histogram 2a: Mean values of Mucosal thickness in different experimental groups



Histogram 3c: Mean values of optical density for IL6 indifferent experimental groups



Histogram 3d: Mean values of +ve PCNA cells number in different experimental groups

DISCUSSION

Potassium bromate (KBrO₃)-induced toxicities are one of society's most serious clinical problems^[30]. It has extensive oxidizing property and mutagenicity. As a parent compound, KBrO₃ is readily taken up from the gastrointestinal tract and expelled mostly in urine; its levels in plasma, erythrocytes, kidney, pancreas, stomach, and small intestine were substantially elevated^[31].

Riboflavin is involved in body development, DNA repair, photosensitization, circadian rhythm, and vitamin activation, including pyridoxine and folate^[32,33].

In this study, KBrO₃-treated group had a highly substantial increase in MDA, which is used as a biomarker for lipid peroxidation, and a significant decrease in the levels of GSH and SOD, indicating cell toxicity. During its biotransformation, KBrO₃ causes toxic insults by producing reactive oxygen species (ROS), which worsen cellular redox balance and structural integrity in the target tissues^[34]. As a strong oxidant, KBrO₃ produces reactive oxygen species (ROS), which causes significant lipid peroxidation and a reduction in GSH levels^[35,36].

A cell's oxidative injury exacerbate peroxidation of membrane-bound lipids, resulting in macromolecule damage, which causes tissue damage and impairment of the body's endogenous antioxidants that prohibit the creation of free radicals^[37,38].

As lipid peroxidation is known to play a crucial role in stomach damage, these results corroborate the histological alterations that occurred in the stomach. KBrO₃ treated group exhibited changes in the fundic gastric mucosa in the form of extravasation of red blood cells in lamina propria, cellular loss and ulceration extending down to muscularis mucosa. When KBrO₃ comes into touch with the tissue surfaces, it is known to disrupt them, it is also readily taken up through the digestive tract., through the blood to cells where ROS are released during its transformation to bromide. Furthermore, biological membranes are degraded by reactive oxygen species^[39]. This might explain why rats exposed to potassium bromate had high ulcer scores and MDA levels. These findings coincided with previous studies of high lipid peroxidation in the organs of rats

exposed to potassium bromate^[40]. These alterations are caused by claudin-1 and zonula occludens-1's affinity for tight junction proteins, resulting in disruption of cell-to-cell connection, inhibition of mitosis, and a decrease in epithelial integrity, resulting in sloughing and desquamation^[41]. KBrO₃ administration caused DNA degradation in treated rats' intestinal tissue, resulting in extensive intestinal damage such as mucosal cell damage, particularly to the membrane^[42].

KBrO₃ increases neutrophil/lymphocyte ratio, this parameter is used to assess the severity of ailments such as peptic ulcers and gastric malignancies for both clinical and experimental scenarios^[43,44]. Also, It activates mast cells in organs of rodents^[45].

Congested blood vessels, and mononuclear cellular infiltrations in the lamina propria were evident in the present study. Inflammatory infiltration may arise from an imbalance between gastrototoxic molecules and the gastric mucosa protection mechanism stimulating the production of tumor necrosis alpha protein and interleukin-1 that, leading to inflammatory cell infiltration to the gastric mucosa^[46]. It could also be due to deterioration of the integrity of the intercellular junction between surface columnar cells as the mucosa has been increasingly exposed to the impacts of acid and proteolytic enzymes, which could be capable of activating neutrophils, lymphocytes, and macrophages^[47]. congested blood vessels were attributed to vasodilator substances released by blood vessels into the blood stream^[50,51].

In the current study, KBrO₃ treated group exhibited vacuolation of the cytoplasm of parietal cells, and the nuclei of parietal and peptic cells were darkly stained. KBrO₃ can trigger an extrinsic pathway of apoptosis, it also triggers intrinsic pathways along with extrinsic as well as ubiquitin/proteasome pathway if it is taken in a higher amount^[48]. These degenerative changes could be explained on the basis of oxidative stress promotes mitochondrial damage and release of cytochrome-c into cytosol^[49].

KBrO₃ treated group exhibited increased amount of collagen fibers between fundic glands, in the lamina propria. Perisinusoidal fibrosis in the liver of rats provided with KBrO₃ was reported^[52], also, it elevated markers including inflammation, angiogenesis, and fibroblast activation. This could be due to mitochondrial damage and dysfunction, which causes cell apoptosis, necrosis, and the activation of a cascade that leads to fibrosis and collagen deposition^[53].

Electron microscopic results confirmed light microscopic study as KBrO₃ treated group revealed mucus neck cell with basal heterochromatic nucleus, wide perinuclear space and apical fused electron lucent secretory mucus granules, the parietal cell appeared with flat heterochromatic nucleus. The cytoplasm contained disturbed tubulovesicular system, degenerated mitochondria and lysosome. Chief cell exhibited peripheral condensation of chromatin of the nucleus with wide

perinuclear space and dilated rough endoplasmic reticulum cisternae. Enteroendocrine cell showed shrunken irregular heterochromatic nucleus, cytoplasmic vacuoles, few small electron dense granules and degenerated mitochondria, similar changes recorded by researchers. They stated that there were many stressors, including the invasion of ROS and toxins into the cell membranes and organelles of the target cells. They also affect the biological activity of macromolecules, resulting in extensive tissue damage and cell dysfunction^[54,55]. The mitochondrial matrix's apoptotic enzymes are released into the cytoplasm leading to cell death^[52]. The early sign of parietal cell damage was disruption of their canaliculi. Dilatation of intracellular canaliculi is due to the stimulation of the cell by histamine leading to re-arrangement of cytoskeleton and engagement of (H⁺/K⁺-ATPase) rich tubulo-vesicles to the apical membrane expanding the intracellular canaliculi with loss of luminal microvilli^[56]. This dilatation occurs in the active phase of secretion. The cytoskeletal actin and phosphorylated ezrin are critical for the development of these histopathological changes, which were essential for fusion of membranes of tubulo-vesicular system with the canaliculi causing its expansion and activation of H⁺/K⁺-ATPase with subsequent gastric acid secretion^[57].

The coalescence of secretory granules was attributed to the increase in the mucus secreted by mucus cells due to increased exocytosis as a response to cell membrane disruption^[58].

Alcian blue (AB) reaction of gastric fundic mucosa of KBrO₃ treated group revealed mild AB reaction in the mucus cells, these results could be due to depletion of Alcian blue stained mucous secretory granules, similar results presented by previous study^[59].

Interleukin-6 (IL-6) is a pleiotropic cytokine that has a role in cancer development, and progression. Oncogene-induced cell transformation and tumorigenesis are both dependent on IL-6. It has a role in tumor initiation^[60]. The mean levels of IL6 increased significantly in the KBrO₃-treated group. It's thought to be a key regulator of acute and chronic inflammation^[61]. It stimulates neutrophils, lymphocytes and macrophages at the target tissue, driving them to create toxic chemicals and lysosomal enzymes that trigger tissue damage in gastric ulcers^[62]. Prior studies have shown that inflamed tissues had substantially enhanced IL-6 mRNA levels^[63,64]. The results of this study showed that KBrO₃ provoked an inflammatory response as evidenced by increased IL-6 immunostaining as a pro-inflammatory cytokine. ROS can lead to inflammation by triggering transcription factors, which cause the creation of similar pro-inflammatory cytokines^[65].

The gastric mucosal cells are continuously undergoing apoptosis and rapidly replaced by newly proliferating cells^[66]. Cellular proliferation plays an essential role in maintaining the integrity of the gastric mucosa. PCNA is an important proliferation marker that is expressed during cell proliferation. A distinctive nuclear staining for PCNA

in rat's liver, after KBrO₃ administration were reported^[67]. DNA oxidation induced by KBrO₃ could occur regardless of lipid peroxidation^[68]. Some researchers reported dysplastic foci in the rats' liver treated with KBrO₃, they stated that the carcinogenicity was established and dependent on both dose- and time^[69].

KBrO₃ and riboflavin treated group showed biochemical improvements paralleled to histological and immunohistochemical findings. As it revealed nearly normal gastric fundic glands similar to control. This came in accordance with the data reported by other researchers who said that riboflavin activate prostaglandin synthesis, mucus and bicarbonate secretion, vascularization of the mucosa, and heightened epithelial cell tolerance to cytotoxic insult while reducing leukocyte recruitment into the fundic mucosa^[70]. Also, riboflavin is a proteasome inhibitor capable of resolving inflammation through reducing the proinflammatory cytokines^[71]. This protective effect of riboflavin is concerned with intrinsic antioxidant potential, causing the oxidative stress and the acute inflammatory response to be attenuated. Moreover, riboflavin is a cofactor for a variety of enzymes concerned with oxidation-reduction processes, as well as a player in protein oxidative folding in the endoplasmic reticulum^[72]. It is a strong free radical scavenger that can neutralize the aggression of the free radicals (ROS) because of the presence of an isoalloxazine ring in its structure. Riboflavin can also exert an antioxidant action through being a component of the glutathione pathway^[73]. Moreover, the current findings revealed that riboflavin administration led to preservation of the proliferative cells of gastric mucosa as indicated in the immunohistochemical results of this work, where this suggested a normal proliferation of cells that kept the gastric mucosa unharmed. Related to this finding, previous studies suggested that riboflavin could act as an anti-proliferative agent in cancerous cells by arresting the cell cycle leading to stop proliferation^[74]. Previous epidemiological studies have demonstrated that riboflavin deficiency has been implicated in aggressive mucosal disorders, which were linked to an increased risk of gastric ulcer and cancer^[75].

According to the previous discussed findings of the present work, it could be concluded that KBrO₃ administration to rats causing significant gastric mucosal changes. These changes could be alleviated by giving riboflavin to maintain the health and integrity of the stomach.

CONFLICT OF INTERESTS

There are no conflicts of interest.

REFERENCES

1. Emeje, M. O., Sabinus, O., Anthony, C. N., Ofoefule, A., & Brown, S. A. (2010): Assessment of bread safety in Nigeria: Quantitative determination of potassium bromate and lead. *African Journal of Food Science*, 4(6), 394–397.

2. Ahmad MK, Zubair H, Mahmood R.(2013): DNA damage and DNA-protein cross-linking induced in rat intestine by the water disinfection by-product potassium bromate. *Chemosphere* 2013; 91: 1221–1224.
3. CSE Study (2016): Potassium Bromate or Potassium Iodate in Bread and Bakery Products (PML/PR-49/2015). www.cseindia.org Analysis of Potassium Bromate in Bread and Flour Samples Sold in Jalingo Metropolis, Northern. DOI: 10.9790/2402-1402010105 www.iosrjournals.org 5 | Page
4. Ekop AS, Obot IB, Ikpatt EN.(2008): Anti-Nutritional Factors and Potassium Bromate Content in Bread and Flour Samples in Uyo Metropolis, Nigerian *E-J Chem.* 5(4), 736-741.
5. Andrzej and Starek-Świechowicz.(2016): Toxicological Properties of Potassium Bromate. *Journal of Pharmacological Reports.* Volume 1 • Issue 3 • 1000122.
6. Wan, J. J., Su, J. F., Sheng, X. L., Shu, T. H., Xing, G. M., Dong, S. X., Hong, M. C., and Ju, Z. (2018): Role of gastroscopic biopsy of gastric ulcer margins and healed sites in the diagnosis of early gastric cancer: A clinical controlled study of 513 cases. *Oncology Letters*, 16(4), 4211– 4218.
7. Iijima, K., Takeshi, K., Yasuhiko, A., Makoto, Y., Sho, A., Motoki, O., Hirota, I., Tomoyuki, K., & Tooru, S. (2016): Preferential location of idiopathic peptic ulcers. *Scandinavian Journal of Gastroenterology*, 51(7), 782–787.
8. Tarasconi, A, Federico, C, Walter, LB, Matteo, T, Luca, A, Edoardo, P, Sarah, M, Vishal, S, Stefania, C, Dieter, G W, Fikri, MA, Fabio, CC. (2020): Perforated and bleeding peptic ulcer: WSES guidelines. *World Journal of Emergency Surgery*, 15(1), 1–24.
9. Said HM, Ross AC, Caballero B, Cousins RJ, Tucker KL, Ziegler TR. (2014): *Modern Nutrition in Health and Disease*. 11th ed. Baltimore, MD: Lippincott Williams & Wilkins; 2014:325-30.
10. Vasileios B, Giovanna A, Maria B, Henrik C. (2018): Safety and efficacy of vitamin B2 for all animal species when used in water for drinking. Volume 16, issue 12, e05531.
11. Erdman JW, Macdonald IA, Zeisel SH. (2012): McCormick DB. Riboflavin. In: *Present Knowledge in Nutrition*. 10th ed. Washington, DC: Wiley-Blackwell:280-92.
12. Balasub S, Christodoulou J, Rahman S.(2019): Disorders of riboflavin metabolism. *J Inher Metab Dis* ;42:608-19.
13. Barile M, Giancaspero TA, Leone P, Galluccio M, Indiveri C.(2016): Riboflavin transport and metabolism in humans. *J Inher Metab Dis* 2016;39:545-57.
14. Mosegaard S, Dipace G, Bross P, Carlsen J, Gregersen N, (2020): Riboflavin Deficiency-Implications for general human health and inborn errors of metabolism. *Int J Mol Sci* 2020;21:E3847.
15. Gaul, C, Diener, HC, Danesch, U. (2015): Improvement of migraine symptoms with a proprietary supplement containing riboflavin, magnesium and Q10: a randomized, placebo-controlled, double-blind, multicenter trial. *J Headache Pain.* 2015; 16: 516.
16. Marashly, ET and Bohlega, SA. (2017): Riboflavin has neuroprotective potential: Focus on Parkinson's disease and migraine. *Front Neurol.* 8:333.
17. Zschabitz S, Cheng TY, Neuhauser ML, Zheng Y, Ray RM, Miller JW. (2013): B vitamin intakes and incidence of colorectal cancer: results from the Women's Health Initiative Observational Study cohort. *Am J Clin Nutr* 97:332-43.
18. Al-Habi, NO, Imam, F, Nadeem, A, Al-Harbi, MM, Iqbal, M, Ahmad, SF.(2014): Carbon tetrachloride-induced hepatotoxicity in rat is reversed by treatment with riboflavin. *Int Immunopharmacol.* 21(2)383-388.
19. Magdy F, Gawish K, Madeha W, and Azza S.(2004): Histological study of the effect of potassium bromate on the thyroid gland of adult male albino rats and the protective role of vitamin C supplement [The].;27(1):180-196.
20. Gloria E, Borgstahl O, Rebecca E. (2018): Superoxide Dismutases(SODs) and SOD Mimetics. *Antioxidants*, 7(11): 156.
21. Saenz-de-Viteri M, Heras-Mulero H, Fernández-Robredo P, *et al.* (2014): Oxidative stress and histological changes in a model of retinal phototoxicity in rabbits. *Oxid. Med, Cell Longev.* 2014;ID 637137.
22. Del Rio D, Stewart AJ, Pellegrini N. (2005): A review of recent studies on malondialdehyde as toxic molecule and biological marker of oxidative stress. *Nutr Metab Cardiovasc Dis.* 15(4):316-28.
23. Suvarna K, Layton C, Bancroft J. (2013): *Theory and Practice of Histological Techniques*, seventh ed. Churchill Livingstone of Elsevier, Philadelphia, USA, pp.173–214.
24. Dykstra K, Michael J, Laura E. (2003): *Biological Electron Microscopy Theory, Techniques, and Troubleshooting* effect of vitamin E and vitamin C. *Pest Biochem Physiol.* 118:10–18.
25. Kiernan, J.A. (2015): *Histological and histochemical methods; Theory and practice*. 5th ed. P.238-390.
26. Dhamia k, Adnan I, Emad K, Abbas and Saad Abudi baqi A. (2017): Immunohistochemistry Analysis for interleukin-6 Expression from the tumor Tissue. *International Journal of Sciences* 3(03).

27. Alfredo De Biasio, Ramon Campos-Olivas, Ricardo Sanchez, Jorge P. (2014): Proliferating Cell Nuclear Antigen (PCNA) interactions in Solution studied by NMR. *PLoS ONE* 9(4):e95818.
28. Nwafor PA, Okwuasaba FK, Binda LG. (2000): Antidiarrhoeal and antiulcerogenic effects of methanolic extract of *Asparagus pubescens* root in rats. *J Ethnopharmacol.* 2000;72(3):421–427. PMID:10996281.
29. Peat J and Barton B. (2005): *Medical statistics. A Guide to data analysis and critical appraisal.* First Edition. Wiley-Blackwell:113-19.
30. Ahmad MK, Khan AA, Ali SN, Mahmood R.(2017): Chemoprotective effect of taurine on potassium bromate-induced DNA damage, DNA-protein cepta L.) peels. *Pakistan Journal of Pharmaceutical Sciences.* 30(5):1971-1979.
31. N. G. Altoom, J. Ajarem, A. A. Allam, S. N. Maooda, and M. A. Abdel-Maksoud,(2018):“Deleterious effects of potassium bromate administration on renal and hepatic tissues of Swiss mice,”*Saudi Journal of Biological Sciences*, vol. 25, no. 2, pp. 278–284, 2018.
32. A. García-Angulo A. (2016):“Overlapping riboflavin supply pathways in bacteria,” *Crit Rev Microbiol*, vol. 43, no. 2, pp. 196–209.
33. G. F. Combs and J. P. McClung, (2017):“Riboflavin,” in *The Vitamins*, pp. 315–329.
34. Tahir, M. U. Rehman, A. Lateef *et al.* (2013):“Diosmin protect against ethanol-induced hepatic injury via alleviation of inflammation and regulation of TNF- α and NF- κ B activation,”*Alcohol*, vol. 47, no. 2, pp. 131–139, 2013.
35. M. U. Rehman, N. Ali, S. Rashid *et al.*(2014):“Alleviation of hepatic injury by chrysin in cisplatin administered rats: probable role of oxidative and inflammatory markers,” *Pharmacological Reports*, vol. 66, no. 6, pp. 1050–1059.
36. DeAngelo, M. H. George, S. R. Kilburn, T. M. Moore, and D. C. Wolf,(2016): “Carcinogenicity of potassium bromate administered in the drinking water to male B6C3F1 Mice and F344/N rats,” *Toxicologic Pathology*, vol. 26, no. 5, pp. 587–594.
37. El-Sokkary GH. (2006): Melatonin protect against oxidative stress induced by the kidney carcinogen potassium bromate. *Neuroendocrinol* 2:461–468. PMID: 11335867.
38. Khan RA, Khan MR, Sahreen S. (2012): Protective effects of rutin against potassium bromate induced nephrotoxicity in rats. *BMCComplement Altern Med* 12:204. doi: 10.1186/1472-6882-12-204.
39. Zhang, X., Dilhara, D. S., Bin, S., Jeffery, F., Richard, J. B., Joseph, A. C., & Cummings, B. S. (2010): Cellular and molecular mechanisms of bromate-induced cytotoxicity in human and rat kidney cells. *Toxicology*,269(1), 13–23.
40. Josiah, S. J., Omotuyi, O., Oluyemi, K. A., Isioma, E., Uhumwangho, E. S., Spencer, C., Nwangwu, O., Olusoji, A. O., & Njoya, H. (2010): Protective role of aqueous extract of *Hibiscus Sabdariffa* (Calyx) against potassium bromate induced tissue damage in wistar rats. *African Journal of Biotechnology*, 9(21), 3218–3222.
41. Vivar, N. and Van Vollenhoven, R.F.(2014):Advances in the treatment of rheumatoid arthritis. *F100Prime Reports*; 6: 31-35.
42. Ahmad M, Khan A, Mahmood R. (2015). Alterations in brush border membrane enzymes, carbohydrate metabolism and oxidative damage to rat intestine by potassium bromate. *Biochimie* 94:2776–2782.
43. Tanrikulu, Y., Tanrikulu, C. S., Sabuncuoglu, M. Z., Kokturk, F., Temi, V., & Bicakci, E. (2016): Is the neutrophil-to-lymphocyte ratio a potential diagnostic marker for peptic ulcer perforation? A retrospective cohort study. *American Journal of Emergency Medicine*, 34(3), 403–406.
44. Yener, M., Mustafa, K. Y., Ozderin, O., Ihsan, A., Ismail, H. K., Zeki, M. Y. K., Mahmut, Y., & Ertugrul, K. (2018): Platelet-to-lymphocyte ratio and neutrophil-to-lymphocyte ratio predict mucosal disease severity in ulcerative colitis *Journal of Medical Biochemistry*, 37(2), 155–162.
45. Semaming, Y., Patchareewan, P., Siriporn, C. C., and Nipon, C. (2015): Pharmacological properties of protocatechuic acid and its potential roles as complementary medicine. *Evidence-Based Complementary and Alternative Medicine*, Vol. 2015, article ID 593902. 11 pages.
46. Konturek, P.C.H.; Duda, A. and Brzozowski, T.(2000): Activation of genes for superoxide dismutase, interleukin-1, tumor necrosis factor- α and intercellular adhesion molecule-1 during healing of ischemia-reperfusion gastric injury. *J. Sc. and Gastroenterol.* 35: 452-463.
47. Ribet, D. and Cossart, P(2015): How bacterial pathogens colonize their hosts and invade deeper tissue. *Microbes and Infection*; 17(3): 173-183.
48. C. M. Bertollo, A. C. P. Oliveira, L. T. S. Rocha, K. A. Costa, E. B. Nascimento Jr., and M. Coelho,(2006):“Characterization of the antinociceptive and anti-inflammatory activities of riboflavin in different experimental models,” *European Journal of Pharmacology*, vol. 547, no. 1-3, pp. 184–191.

49. McInnes, IB, Schett, G.N, and Engl, J.(2011): The pathogenesis of rheumatoid arthritis. *Med.* 2011; 365(23): 2205-2219.
50. Lundgren, J. and Radegran, G. (2014): Pathophysiology and potential treatments of pulmonary hypertension due to systolic left heart failure. *Acta Physiol (Oxf)*; 211 (2):314-333.
51. Gheth, E. M., Eldurssi, I. S., Algassi, A. A., Abdalla, G. M., and Hamad, M. A. (2019): Histopathological effects of potassium bromate on liver male rat's and possible protective role of ruta chalepensis L. (Rutaceae) oil extract. *Asian Journal of Pharmaceutical Research and Development*, 7, 93–97.
52. Dimkpa, U., Ukoha, U., Anyabolu, E., Uchefuna, R., Anikeh, L., Oji, O. Emenjo, O. (2013): Hepatotoxic effects of potassiumbromate on adult wistar rats. *Journal of Biology, Agriculture and Healthcare*, 3, 111–115.
53. Duval F, Moreno-Cuevas JE, Gonz_alez-Garza MT, Rodr_iguez- Montalvo C, Cruz-Vega DE. (2014): Liver fibrosis and protectionmechanisms action of medicinal plants targeting apoptosis of hepatocytesand hepatic stellate cells. *Adv Pharmacol Sci* 2014:373295.
54. Akanji MA, Nafiu MO, Yakubu MT. (2008): Enzyme activities andhistopathology of selected tissues in rats treated with potassiumbromate. *Afr J Biomed Res* 11:87–95. doi.org/10.4314/ajbr.v11i1.50672.
55. A. Starek and B. Starek-Świechowicz,(2016):“Toxicological propertiesof potassium bromate,” *Journal Pharmaceutical Reports*,vol. 1, p. 3.
56. Ogata, T. and Yamasaki, Y. (2000): Morphological studies on the translocation of tubulovesicular system toward the intracellular canaliculus during stimulation of the gastric parietal cell. *J. Mic. Res. Tech*; 48: 282- 292.
57. Wakamatsu, D.; Tsuyama, S.; Maezono, R.; Kato, K.; Ogata, S.; Takao, S.; Natsugoe, S.; Aikoe, T. and Murata, F.(2005): Immunohistochemical Detection of the Cytoskeletal Components of the Gastric Parietal Cells. *Acta Histochem. Cytochem.* 2005; 38(5): 331-337.
58. Miyake, K.; Tanaka, T. and McNeil, P.L. (2006): Disruption-induced mucus secretion. Repair and Protection. *J. PLOS. Biol.* 4(9): 276-282.
59. Ahmad, K. M., & Mahmood, R. (2015): Oral administration of potassium bromate, a major water disinfection by-product, induces oxidative stress and impairs the antioxidant power of rat blood. *Chemosphere*, 87(7), 750–756.
60. Iliopoulos D, Hirsch HA, Struhl K. (2009): An epigenetic switch involving NF-kappaB, Lin28, Let-7 MicroRNA, and IL6 links inflammation to cell transformation. *Cell* 139: 693–706.
61. D. Kamimura, Y. Arima, T. Hirano, H. Ogura, M. Murakami. (2014): IL-6 and inflammatory diseases, *Cytokine Front.* Springer; 53–78.
62. A.-A. Karolin Kamel. (2011): Comparative evaluation of the anti-ulcer activity of curcumin and omeprazole during the acute phase of gastric ulcer efficacy of curcumin in gastric ulcer prevention against omeprazole, *Food and Nutrition Sciences*. Vol. 2 No. 6,article ID 6622.
63. T. Kishimoto. (2010): IL-6: from its discovery to clinical applications, *Int. Immunol.* dxq030.
64. Stenvinkel, P., Ketteler, M., & Johnson, R. J. (2005): IL-10, IL-6, and TNF alpha: central factors in the altered cytokine network of uremia —the good, the bad, and the ugly. *Kidney International*, 67, 1216 –1233.
65. Valério, D. A., Georgetti, S. R., Magro, D. A., Casagrande, R., Cunha, T. M., Vicentini, F. T., *et al.* (2009): Quercetin reduces inflammatory pain: inhibition of oxidative stress and cytokine production. *Journal of Natural Products* , 72, 11975 –11979.
66. Szabo, I., and Tarnawski, A. S. (2000): *J PhysiolPharmacol* 51, 3-15.
67. Elmahdy, M. M., Moussa, E., Sherein, M. A.-E., & Alwazaan, A. (2015): Pathological and Immunohistochemical study of potassium bromated on the liver of rat. *The Veterinary Medical Journal-Giza*, 2, 73–82.
68. Umemura T, Tasaki M, Kijima A, Okamura T, Inoue T, Ishii Y, Suzuki Y, Masui N, Nohmi T, Nishikawa A (2009):Possible participation of oxidative stress in causation of cell proliferation and in *in vivo* mutagenicity in kidneys of gpt delta rats treated with potassium bromate. *Toxicology* 257:46–52.
69. Shi, Q. Yang, X. Greenhaw, J. and Salminen, W.(2011): Hepatic Cytochrome P450s Attenuate the Cytotoxicity Induced by Leflunomide and Its Active Metabolite A77 1726 in Primary Cultured Rat Hepatocytes. *Toxicological Sciences*. 122(2): 579–586.
70. Martin, and Wallace, JL. (2006): Gastrointestinal inflammation: a central component of mucosal defense and repair. *Exp Biol Med.* 231: 130–137.
71. Qureshi, AA, Tan, X, Reis, JC, Badr, MZ, Papasian, CJ, Morrison, DC, Qureshi, N.(2011): Suppression of nitric oxide induction and pro-inflammatory cytokines by novel proteasome inhibitors in various experimental models. *Lipids Health Dis.* 10: 177.
72. Tu, BP, Ho-Schleyer, SC, Travers, KJ, Weissman, JS.(2000):. Biochemical basis of oxidative protein folding in the endoplasmic reticulum. *Science.* 290: 1571-1574.

73. Ashoori, M and Saedisomeolia.(2014): A Riboflavin (vitamin B2) and oxidative stress: a review. *Br J Nutr.* 111(11):1985-1891.
74. de Souza Queiroz, KC, Zambuzzi, WF, Santos de Souza, AC, da Silva, RA, Machado, D, Justo, GZ, Carvalho, HF, Peppelenbosch, MP, Ferreira, A.(2007): possible anti-proliferative and anti-metastatic effect of irradiated riboflavin in solid tumours. *Cancer Lett.* 2007; 258(1):126-134.
75. Matnuri, M, Zheng, C, Sidik, D, Bai, G, Abdukerim, M, Abdukadier, A Ahmat, K, Ma, Y, Eli, M.(2015): Correlation analysis of riboflavin, RFT2 and *Helicobater pylori* in gastric carcinoma. *Int J Clin Exp Pathol.* 8(10):13339-13345.

الملخص العربي

دراسة هستولوجية وهستوكيميائية على تأثير برومات البوتاسيوم على الغشاء المخاطي لقاع معدة ذكور الجرذان البيضاء البالغة والتأثير التحسني المحتمل للريبوفلافين

اميرة فهمي علي، سهام احمد محمد عبد العزيز، رانيا سعيد عماره

قسم الأنسجة، كلية الطب؛ جامعة المنوفية، مصر

الخلفية: يعتبر برومات البوتاسيوم عامل مؤكسد قوي يستخدم كمحسن للدقيق، وله تأثيرات مسرطنة وقد يتسبب في حدوث بعض الطفرات من خلال توليد جزيئات الأكسجين التفاعلية الحرة. كما يعرف برومات البوتاسيوم بتسببه في تهيج الأنسجة التي تتلامس معه. الريبوفلافين له دور حيوي في الوظائف الخلوية والنمو. كما ان له تأثير قوي مضاد للأكسدة ومضاد للالتهابات ومعدلة للمناعة.

الهدف من البحث: تهدف هذه الدراسة لتقييم تأثير برومات البوتاسيوم على الغشاء المخاطي لقاع ذكور الجرذان البيضاء البالغة والتأثير الوقائي المحتمل للريبوفلافين .

المواد وطرق البحث: تم استخدام أربعين من ذكور الجرذان البيضاء البالغة، مقسمة إلى أربع مجموعات ، المجموعة الأولى (المجموعة الضابطة) ، المجموعة الثانية (المجموعة المعالجة بالريبوفلافين) ، المجموعة الثالثة (المجموعة المعالجة بالبوتاسيوم برومات) والمجموعة الرابعة (المجموعة المعالجة بالبوتاسيوم برومات والريبوفلافين) ، بعد ٢٤ ساعة من الجرعة الأخيرة من تناول الأدوية ، تم الحصول على أنسجة المعدة ومعالجتها للدراسات البيوكيميائية والنسجية والكيميائية النسيجية والكيميائية المناعية.

نتائج البحث: أظهرت المجموعة المعالجة ببرومات البوتاسيوم تدهوراً ملحوظاً في الغشاء المخاطي لقاع المعدة حيث ظهر في مساحة واسعة من النسيج الظهاري مع فقدان الخلايا السطحية ، وظهرت الخلايا الجدارية والرئيسية بأنوية صغيرة وغامقة كما ظهرت أوعية دموية محتقنة وتجمع للخلايا الالتهابية وحيدة النواة. ولوحظ اتساع في الشبكة الإندوبلازمية الخشنة وحبيبات افرازيه متكدسه في الخلايا الرئيسية. احصائياً، هناك زيادة ملحوظة ذات دلالة في متوسط مساحة ترسب ألياف الكولاجين، وزيادة في القيم المتوسطة للكثافة الضوئية للانترلوكين ٦ ، ومتوسط عدد الخلايا الايجابية لصبغة بيكنا. وقد تحسنت التغيرات السابق ذكرها بعد اضافة الريبوفلافين.

الخلاصة: يؤثر برومات البوتاسيوم على الغشاء المخاطي لقاع المعدة ، ويمكن تخفيف هذه التأثيرات عن طريق تناول المتزامن للريبوفلافين.